A CHO stable pool production platform for rapid clinical development of trimeric SARS-CoV-2 spike subunit vaccine antigens

Joubert, Simon; Stuible, Matthew; Lord-Dufour, Simon; Lamoureux, Linda; Vaillancourt, François; Perret, Sylvie; Ouimet, Manon; Pelletier, Alex; Bisson, Louis; Mahimkar, Rohan; Pham, Phuong Lan; L'Ecuyer-Coelho, Helene; Roy, Marjolaine; Voyer, Robert; Baardsnes, Jason; Sauvageau, Janelle; St-Michael, Frank; Robotham, Anna; Kelly, John; Acel, Andrea; Schrag, Joseph D.; El Bakkouri, Majida; Durocher, Yves

Publisher's version / Version de l'éditeur:
https://doi.org/10.1002/bit.28387
Biotechnology and Bioengineering, 120, 7, pp. 1746-1761, 2023-07

Received: 17 January 2023 | Revised: 2 March 2023 | Accepted: 14 March 2023

DOI: 10.1002/bit.28387

ARTICLE

BIOTECHNOLOGY AND BIOENGINEERING WILEY

A CHO stable pool production platform for rapid clinical development of trimeric SARS-CoV-2 spike subunit vaccine antigens

Simon Joubert[1] | Matthew Stuible[1] | Simon Lord-Dufour[1] | Linda Lamoureux[1] | François Vaillancourt[1] | Sylvie Perret[1] | Manon Ouimet[1] | Alex Pelletier[1] | Louis Bisson[1] | Rohan Mahimkar[1] | Phuong Lan Pham[1] | Helene L'Ecuyer-Coelho[1] | Marjolaine Roy[1] | Robert Voyer[1] | Jason Baardsnes[1] | Janelle Sauvageau[2] | Frank St-Michael[2] | Anna Robotham[2] | John Kelly[2] | Andrea Acel[1] | Joseph D. Schrag[1] | Majida El Bakkouri[1] | Yves Durocher[1,3]

[1]Human Health Therapeutics Research Centre, National Research Council Canada, Montréal, Québec, Canada

[2]Human Health Therapeutics Research Centre, National Research Council Canada, Ottawa, Ontario, Canada

[3]Department of Biochemistry and Molecular Medicine, Faculty of Medicine, Université de Montréal, Montréal, Québec, Canada

Correspondence
Yves Durocher, Human Health Therapeutics Research Centre, National Research Council Canada, 6100 Royalmount Ave, Montréal, QC H4P 2R2, Canada.
Email: yves.durocher@nrc-cnrc.gc.ca

Abstract

Protein expression from stably transfected Chinese hamster ovary (CHO) clones is an established but time-consuming method for manufacturing therapeutic recombinant proteins. The use of faster, alternative approaches, such as non-clonal stable pools, has been restricted due to lower productivity and longstanding regulatory guidelines. Recently, the performance of stable pools has improved dramatically, making them a viable option for quickly producing drug substance for GLP-toxicology and early-phase clinical trials in scenarios such as pandemics that demand rapid production timelines. Compared to stable CHO clones which can take several months to generate and characterize, stable pool development can be completed in only a few weeks. Here, we compared the productivity and product quality of trimeric SARS-CoV-2 spike protein ectodomains produced from stable CHO pools or clones. Using a set of biophysical and biochemical assays we show that product quality is very similar and that CHO pools demonstrate sufficient productivity to generate vaccine candidates for early clinical trials. Based on these data, we propose that regulatory guidelines should be updated to permit production of early clinical trial material from CHO pools to enable more rapid and cost-effective clinical evaluation of potentially life-saving vaccines.

KEYWORDS

CHO clones, CHO pools, product comparability, quality attributes, SARS-CoV-2 spike protein

Simon Joubert and Matthew Stuible are joint first authors.

1 | INTRODUCTION

Improving the yield and quality of recombinant proteins produced by Chinese hamster ovary (CHO) cells has been the subject of intense research since the first CHO-derived product, alteplase tissue plasminogen activator (tPA), was approved for therapeutic use in 1987 (Semba et al., 2001). During subsequent decades, different groups, including nearly every major pharmaceutical company involved in biologics development, have been developing and optimizing their own CHO-based expression platforms. The diversity of these platforms is notable, including differences in choice of CHO cell lineages, expression plasmid constructs, gene transfer and selection methods, culture media, and cell and process engineering strategies (Coulet et al., 2022; Donaldson et al., 2022; Durocher & Butler, 2009; Reyes et al., 2022; Wurm, 2013; Wurm & Wurm, 2017). However, a common feature has been the mandatory use of stable clonal cell lines for both clinical development and manufacturing, a result of several factors including longstanding regulatory guidelines (Stuible et al., 2018). With recent and significant improvements in performance, alternative non-clonal platforms, including stably transfected CHO pools and transient gene expression, are now capable of producing recombinant proteins more rapidly and cost-effectively with yields and quality similar to clonal cell lines (Fan et al., 2017; Hu et al., 2017; Munro et al., 2017; Rajendra et al., 2017; Rodriguez-Conde et al., 2022; Scarcelli et al., 2017; Wright et al., 2017; Ye et al., 2010). Such methods may now be in a unique position to facilitate rapid clinical evaluation of novel, life-saving protein-based biologics.

The COVID-19 pandemic has propelled the use of non-clone-derived material for clinical trials from a theoretical possibility towards widespread adoption by industry. The application of different stable CHO pool technologies for rapid production of SARS-CoV-2 neutralizing antibodies used in clinical trials was reported recently by Merck KGaA, Junshi Biosciences, and Wuxi Biologics (Agostinetto et al., 2022; Tan et al., 2022; Xu et al., 2022; Zhang et al., 2021). Eli Lilly, Regeneron, and AstraZeneca have also publicly disclosed their use of non-clonal CHO-based methods for similar purposes, although not in peer-reviewed publications (McGovern et al., 2022). Finally, Boehringer Ingelheim and Catalent Pharma Solutions also recently described details of similar platforms, although details of the protein product including clinical indication were not disclosed (Hall et al., 2022; Schmieder et al., 2022). There appears to have been a common understanding that in response to a global health emergency such as COVID-19, it was unacceptable to delay human trials for the sake of undertaking lengthy monoclonal CHO cell line isolation.

One presumable risk of using a pool approach is that it can produce a heterogeneous or inconsistent product from batch to batch. Nowadays, this risk can be significantly mitigated by using modern and sensitive analytical tools such as LC-MS for product analyses and by implementing more stringent manufacturing control strategies, for example, by initiating every production from a single lot of cryopreserved cell vials and by using tightly controlled, robust and reproducible upstream and downstream processes. The experiences reported by multiple companies during the pandemic provide ample evidence that non-clonal methods can provide monoclonal antibody drug substance of sufficient quality, quantity, and safety for first-in-human trials. This should allow the possibility for clonal cell line generation, which is nonetheless still required for later clinical phases and product manufacturing, to be taken off the critical path to clinical development.

Methods to generate stable, recombinant protein-expressing CHO cells are commonly based on transfection of plasmid vectors encoding the transgene of interest and a selectable marker (e.g., glutamine synthase [GS], dihydrofolate reductase [DHFR] or an antibiotic resistance gene) followed by a drug selection step that selects for cells that have stably integrated the plasmid in their genome. Selection of high-producing clones from this type of stable pool has historically been the basis of most CHO clone development workflows. A perceived drawback of this "random integration" approach is the lack of control over how and where transfected plasmids are inserted in the CHO genome: poor transgene expression may result from integration of plasmids into non-optimal loci or of plasmid fragments that contain the selectable marker without the transgene cassette. As a result, interest in targeted integration methods, including transposase-mediated integration (Balasubramanian et al., 2015; Matasci et al., 2011) and recombinase-mediated cassette exchange (RMCE) has been growing, both of which are capable of generating highly productive pools (Srirangan et al., 2020). Notably, among the recent reports describing the use of non-clonal pools to produce recombinant proteins for clinical trials, the majority have used transposase- or RMCE-based methods for pool generation (Agostinetto et al., 2022; Schmieder et al., 2022; Zhang et al., 2021).

Despite this recent trend, our experience with CHO stable pools generation suggested that the random integration approach can also give very good and consistent yields of high-quality recombinant proteins that could be appropriate for early-stage clinical trials. Importantly, we believe that random-integrated pools are a more accessible technology: unlike targeted integration methods, they do not require proprietary transposases/recombinases or long and tedious prior identification and validation of genomic RMCE loci. Our random integration stable pool platform is based on the CHO$^{2353™}$ cell line, a CHO-DXB11-derived clone expressing the reverse cumate transactivator (rcTA). These cells support both inducible and constitutive transgene expression, under control of an engineered CR5 promoter, depending on whether a cumate-regulated repressor (CymR) is co-expressed or not. Previously, we and others have shown that the ability to down-regulate transgene expression during pool selection can improve their productivity later during the production phase (Lam et al., 2017; Misaghi et al., 2014; Ong et al., 2019; Poulain et al., 2019); the ability to evaluate both expression modes (constitutive and inducible) using the same host cell line is a unique feature of our platform.

In response to the COVID-19 pandemic, an important focus of our research has been the production of recombinant SARS-CoV-2 spike proteins in CHO cells. These proteins, specifically soluble, trimeric, prefusion-stabilized spike ectodomain constructs (Stuible

et al., 2021), have been investigated as candidate vaccine antigens and also as reagents for serosurveillance studies (Akache et al., 2021, 2022; Chisanga et al., 2022; Colwill et al., 2022; Rudi et al., 2022; Stark et al., 2022; Stocks et al., 2021). With the frequent emergence of new variants, we have had the opportunity to generate dozens of spike-expressing CHO pools over the last 2 years, which has allowed us to appreciate better the performance and robustness of this expression platform. Spike protein expression was consistently higher (by 2- to 5-fold) in cumate-inducible compared to constitutive pools, achieving yields of 200–700 mg/L for all variants tested. For one of the variants (B.1.617.2, or Delta), we also derived cumate-inducible clonal cell lines, the best of which reached yields of 2.0 g/L. Notably, expression stability over many cell doubling times (>40) was similar for pools and the derived clones. Finally, we evaluated several quality attributes of spike proteins purified from clones and stable pools, including protein size distribution by analytical size-exclusion chromatography (SEC), thermal stability by differential scanning calorimetry (DSF), N- and C-terminal sequence identity by LC-MS, glycosylation by high-performance anion exchange chromatography with pulsed amperometric detection (HPAEC-PAD), and ACE2 binding by surface plasmon resonance (SPR). These results indicate a high degree of similarity between pool- and clone-derived materials, although slight variations in some of these attributes could be detected in proteins purified from some specific clones. The material from pools tended to be well-representative of the average clone-derived product, with many clones matching very closely pool-derived product attributes. Overall, the extensive testing of the CHO^{2353} stable pool platform described here supports the potential of such pools to expedite early-phase clinical testing of novel recombinant protein therapeutics.

2 | MATERIALS AND METHODS

2.1 | Plasmid vectors

Spike protein-coding sequences in plasmid vectors used to prepare stably transfected pools were CHO codon-optimized and included the full ectodomain of the SARS-CoV-2 spike protein with prefusion-stabilizing "2P" and furin-site mutations (Sm), fused to human resistin ("T1") or T4 fibritin (foldon, "T2") trimerization sequences, as described previously (Stuible et al., 2021). The SmT1 construct contains C-terminal FLAG-His affinity tags while all other constructs are tagless (indicated by "v3" annotation). The pTT81® plasmid used to generate constitutive-expression pools is based on pTT109® (Joubert et al., 2022) but contains only one expression cassette with a CR5 promoter for expression of a single polypeptide. For inducible-expression pools, the pTT241® expression plasmid was generated from pTT81 by adding an expression cassette for CymR. The pTT180®-rcTA plasmid is identical to the pTT54®-rcTA plasmid described before (Poulain et al., 2017) except that the puromycin resistance gene was replaced by the DHFR gene to confer resistance to methotrexate and a SV40 large T antigen nuclear localization signal was added to the N-terminus of the CymR protein. Spike protein sequences were codon-optimized for *Cricetulus griseus* and synthetized by GenScript as described previously (Stuible et al., 2021). All plasmids were amplified in *Escherichia coli* (DH5α) and purified using an in-house low-endotoxin chromatographic method (unpublished). DNA pellets were dissolved in sterile endotoxin-free TE buffer and quantified by measuring absorbance at 260 and 280 nm, before confirmation of the plasmid sequence by DNA sequencing.

2.2 | Cell lines and culture conditions

The CHO^{2353}™ cell line used in this study was selected as follows: parental CHO-DXB11 cells were thawed in PowerCHO-2 CD medium (Lonza) containing 4 mM of L-Glutamine (Hyclone) and then transfected in CD-DG44 medium (Life Technologies) using linear polyethylenimine hydrochloride Max (PEI MAX, Polysciences) complexed with pTT180-rcTA plasmid DNA. The transfected cells were selected using 150 nM Methotrexate (MTX, Sigma-Aldrich) for 2 weeks and then sorted using FACS (MoFlo Astrios EQ, Beckman Coulter) to generate monoclonal cell lines. Cell lines were screened for expression of a recombinant protein following transfection of a plasmid containing the cDNAs of interest under the control of the CR5 promoter. Clone 2353 was selected as the best producer cell line; it can be used for both constitutive and inducible expression of proteins. For constitutive expression, cells are transfected with the pTT81 plasmid containing the gene of interest under control of the CR5 promoter. The constitutive expression of the rcTA transactivator in the CHO^{2353} cell line drives constitutive expression of the gene of interest through the CR5 promoter. For inducible expression, cells are transfected with the pTT241 plasmid which also contains a cassette for constitutive expression of the CymR repressor. In this context, CymR binds and blocks both the CMV5CuO promoter driving rcTA expression and the CR5 promoter through binding to the CuO operators, thus significantly reducing expression of the gene of interest. Adding the small molecule inducer cumate (p-isopropylbenzoate) results in its binding to the CymR repressor, which induces a conformational change that reduces its binding affinity for the CuO operators and allows the rcTA to drive gene expression from the CR5 promoter. Cell lines were cultured in chemically defined, animal component-free BalanCD CHO Growth A medium (FUJIFILM Irvine Scientific) supplemented with 4 mM L-Glutamine (Hyclone) and 0.125% (v/v) Anti-clumping Agent A (Lonza). Cells were maintained at 37°C and 5% CO_2 under constant agitation (120 rpm) and passaged three times per week at a cell density of 0.1×10^6 to 0.2×10^6 cells/mL, with a maximal viable cell density (VCD) of 2×10^6 cells/mL in 125 mL or 250 mL Erlenmeyer flasks (Corning), with 25- or 50-mL culture medium, respectively. VCD and viability were measured either with the Cedex Analyzer automated cell counter (Roche) or with a Vi-CELL XR cell counter (Beckman Coulter) using the trypan blue exclusion method.

2.3 | Generation of stable CHO cell pools

CHO$^{2353™}$ cells were cultured as described in the previous section for at least 8 days before stable pool generation. The day of transfection, the cell suspension was analyzed using an automated cell counter, and to be qualified, a VCD of $2.0 \pm 0.5 \times 10^6$ cells/mL with a viability greater than 98% was required. Before transfection, a complete media change by centrifugation was performed using BCDT-Complete (BalanCD Transfectory CHO chemically defined medium supplemented with 4 mM L-Glutamine and 0.1% (w/v) Kolliphor P188). Cells were resuspended in BCDT-Complete at 2.0×10^6 cells/mL and incubated at 37°C, 5% CO_2 and 120 rpm for at least 1 h. For transfection, DNA/polyethylenimine polyplexes were prepared by prediluting plasmid DNA and PEI MAX separately in a volume of BCDT-Complete corresponding to 1/20 of the final transfected culture volume. The diluted DNA was mixed with the diluted PEI MAX and incubated at room temperature for 3–5 min. Polyplexes were then added to the preprepared cell suspension. Final concentrations of DNA and PEI MAX were 1 and 5 µg/mL, respectively. The transfected cell suspension was then incubated at 37°C, 5% CO_2 and 120 rpm for 24 h before starting the selection phase. For MSX selection, a complete media change was performed by centrifugation of the transfected cell suspension and resuspension at 0.5×10^6 cells/mL in PowerCHO2 media supplemented with 50 µM of MSX and 0.125% (v/v) of Anti-clumping Agent A. The cell suspension was analyzed every 2–3 days using an automated cell counter. Until 90% cell viability was reached, a complete media change was performed, as above, into fresh selection media. At > 90% viability, media change was not performed and the cell suspension was directly diluted at 0.3×10^6 cells/mL in the selection media. The stable pool generation process was considered to be complete when viability was above 98% with a steady doubling time for at least two passages, usually at around 18–20 days posttransfection. Finally, the selected stable pool was centrifuged and cryopreserved at 15×10^6 cells/mL in 1 mL of PowerCHO2 media supplemented with 7.5% (v/v) DMSO Hybri-Max (Sigma-Aldrich) per cryovial. Using a CoolBox (BioCision), cryovials were immediately transferred at −80°C for at least 24 h and subsequently moved to a liquid nitrogen tank for long-term storage.

2.4 | Fed-batch culture production

CHO cell pools and clones were thawed at least 8 days before starting productions in BalanCD Growth A chemically defined medium supplemented with 50 µM of MSX and 0.1% (w/v) Kolliphor P188. Production cultures were inoculated either in 50–1500 mL shake flasks (Corning) or in 6-well extradeepwell plates (Enzyscreen) 3 days before induction and incubated at 37°C, 5% CO_2 under constant agitation at 120 rpm; inoculation cell density was variable (calculated based on culture doubling time with a target VCD of at least $5.0 \pm 0.5 \times 10^6$ cells/mL). Expression of the recombinant protein was induced by adding 2 µg/mL of cumate. Cumate was purchased from Ark Pharm Inc. and dissolved at 2 mg/mL in 95% (v/v) ethanol. At the same time, BalanCD CHO Feed 4 (FUJIFILM Irvine Scientific) was added and culture temperature was shifted to 32°C. Every 2–3 days, cultures were analyzed using an automated cell counter, fed with Feed 4 according to a predefined regimen and samples were collected to measure glucose concentrations (VITROS 350, Orthoclinical Diagnostics). When needed, glucose was added to maintain a minimal concentration of 17 mM between each sampling time point. At 10 days posttemperature shift, the fed-batch production cell suspension was harvested by centrifugation at $3300 \times g$ for 25 min at RT followed by a 0.22 µm filtration step using a Millipore filtration unit. The clarified supernatant was stored no longer than 4 days at 4°C before analysis and purification.

2.5 | Analysis and quantification of spike protein by SDS-PAGE

Purified recombinant SARS-COV-2 spike protein serial dilutions as well as various volumes of clarified production supernatants were loaded simultaneously on a precast TGX stain-free gel (Bio-Rad) using 4X Laemmli sample buffer (Bio-Rad) supplemented with 200 mM DTT (Bioshop). Before loading, all diluted samples were heated at 70°C for 10 min. Following sample separation at 200 V for 35 min in TGX running buffer (Bio-Rad), gels were UV-activated and then visualized using a ChemiDoc MP Imaging system (Bio-Rad). Then, densitometry analysis was performed with Image Lab software (Bio-Rad). The production volumetric titer estimation (mg/L) was then obtained by dividing the back-calculated spike quantity per well (based on the purified protein standard curve) by the volume of clarified production supernatant loaded.

2.6 | Spike protein purification

Supernatants containing the spike protein were filtered using 0.22 µm steriflip (Millipore) and loaded onto DPBS-equilibrated columns of NGL COVID-19 Spike Protein Affinity Resin (Repligen) by gravity flow. Clarified supernatants containing approximately 5 mg of spike protein were loaded on columns containing a packed resin volume of 2 mL. Columns were washed with 5 CV of DPBS and eluted with 100 mM sodium acetate pH 3.5. Purified proteins were formulated in DPBS pH 7.8 at protein concentrations not exceeding 2 mg/mL by buffer exchange through NAP-25 desalting columns (Cytiva), filter-sterilized using Millex-GV 0.22 µm syringe filters (Millipore) and stored at −80°C. Concentrations of purified proteins in DPBS were determined by spectrophotometry (A_{280}) using extinction coefficients calculated based on their amino acid composition.

2.7 | Generation of CHO clones expressing Delta SARS-CoV-2 spike protein

Stable CHO pool expressing SARS-CoV-2(Delta) spike protein was cultured in BalanCD CHO Growth A medium supplemented with 50 µM MSX and 0.125% (v/v) Anti-clumping Agent A. Two hours

before FACS sorting, 384-well plates were prefilled with BalanCD CHO Growth A medium supplemented with 0.22 µm-filtered ClonaCell-CHO ACF Supplement (STEMCELL Technologies) and kept at 37°C, 5% CO_2 in a controlled atmosphere. Four million cells were centrifuged at 220 × *g* for 5 min at room temperature, resuspended in BalanCD CHO Growth A at 2×10^6 cells/mL and plated in 6-well plates (NUNC). Cells were then labeled for 20 min with 2 µM of CellTracker Orange CMRA (ThermoFisher) and sorted using FACS (MoFlo Astrios EQ, Beckman Coulter) at 1 cell/well in 8 × 384-well plates. The sort was performed using single sort mode and 0.5 drop envelop parameters. Following cell sorting, plates were centrifuged immediately at 1200 × *g* for 5 min at room temperature and scanned on ImageXpress micro XLR (Molecular Devices) using a protocol that uses Transmitted Light and Texas Red channels. The Texas Red channel allows visualization of CellTracker Orange stained cells and permits better verification of monoclonality than the Transmitted Light image alone. One day postsorting, the plates were scanned again using transmitted light only to follow the cell growth. Thirteen days postsorting, the plates were scanned again using transmitted light only to evaluate outgrowth and confluency. Nine hundred and sixty outgrown clones were kept and evaluated for expression of spike protein in static 96-well plates using an Octet RED96-based spike quantitation assay. The top 96 clones were expanded in 96-well deepwell plates and cryopreserved. The top 42 clones were then expanded in 6-well deepwell plates (Corning) cultured in BalanCD CHO Growth A medium supplemented with 50 µM MSX and 0.125% (v/v) Anti-clumping Agent A, before cryopreservation of each cell line into cryovials at 10×10^6 cells in 1 mL per cryovial, in BalanCD CHO Growth A medium supplemented with 7.5% (v/v) DMSO. This was followed by evaluation of expression stability of the clones in 6-well extradeepwell plates (Enzyscreen). Productivity was determined in fed-batch at a reference time point (after 28 population doublings), after which only the top 18 clones were kept for further evaluation of productivity in fed-batch at two additional time points (after 67 and 96 population doublings).

2.8 | Production and stability of SmT1v3 reference-strain pool in 0.75 L bioreactors

Stable CHO pool expressing SmT1v3 (reference variant) was thawed in BalanCD CHO Growth A medium supplemented with 0.1% (w/v) Kolliphor P188 and 50 µM MSX. Cells were passaged every other day (or 3 days for the weekend) in flask shaken at 120 rpm located in 5% CO_2 incubator at 37°C with >70% relative humidity. Cells were maintained in the logarithm growth phase with a typical doubling time of 18–20 h. Seed trains at passage 5 (~11 generations), passage 8 (~21 generations), and passage 11 (~31 generations) were used to inoculate 0.75 L Multifors 2 bench-scale bioreactors (Infors HT, max working volume of 0.75 L, nominal [total] bioreactor volume of 1 L). The six 0.75 L Multifors 2 bioreactors were used to investigate scalability and the effect of cell passage number in bioreactor. The initial working volume was 0.6 L. A fed-batch cell culture using the BalanCD CHO Feed 4 was conducted after 3 days of cell growth at 37°C using a 2- and 3-day feed with a total feed volume of 32.5% (v/v; feed volume was calculated based on the initial working volume). Typically, bioreactors were inoculated at 0.4×10^6 cells/mL. Cells were grown at 37°C for 3 days. pH was initially set at 7.05 ± 0.05 for 2 days then was shifted to 6.95 ± 0.05. pH was regulated by sparging CO_2 or adding base solution (4% NaOH; 9% $NaHCO_3$). Three days after inoculation, cells routinely reached $4–5 \times 10^6$ cells/mL. Cumate was added to the bioreactor at a concentration of 2 µg/mL. BalanCD CHO Feed 4 was added as required followed by a temperature shift to 32°C. The Multifors bioreactors contained two pitched-blade impellers and a microsparger (10 µm diameter). A sparge Air/Oxygen cascade together with air overlaying strategy was developed to control the DO setpoint of 40% (of air saturation) throughout the experiment. Agitation speed was set at 165 rpm which corresponds to a power input (P/V) of 35 Watts/m^3. Antifoam (FoamAway, ThermoFisher) was added 3 days postinoculation (0.1%, v/v) or as needed afterward. Sampling was conducted daily during the 3-day growth phase at 37°C then at every feed event during the fed-batch production phase. Cell count was done using a Vi-CELL BLU cell counter (Beckman Coulter) and Trypan blue dye exclusion method. Key metabolites such as glucose, lactate, and ammonia were monitored using the Vitros 350 Chemistry System (Orthoclinical Diagnostics). Online monitoring of 3-gas flowrates (air, oxygen, and carbon dioxide), DO, pH, agitation rate, temperature, and base volume addition was conducted during the production run using the BioAnalyst software (BioIntelligence Inc.). 2 M glucose solution (Sigma-Aldrich) was added based on daily glucose consumption rate of the previous sampling point to ensure a minimal level of 17 mM glucose at the next time point. Centrifuged supernatant samples were stored at −80°C for product yield measurement at the end of the experiment using TGX Stain-free SDS-PAGE gels (Bio-Rad) as described above.

2.9 | Bio-layer interferometry spike protein quantitation assay

Quantification on the Octet-RED96 (FortéBio) was performed using 96-well plates (Evergreen) and Protein A probes (Sartorius). Assay buffer was composed of 10X Kinetic buffer (Sartorius) diluted 10-fold in DPBS (Hyclone). Assay buffer was used to make the matrix solution and to dilute samples. The matrix solution was composed of conditioned media diluted 1 in 3 in assay buffer. The matrix was used to rehydrate probes, dilute the standards and controls, and as neutralization solution. Regeneration solution was composed of 10 mM glycine (Sigma-Aldrich) with pH adjusted to 1.1 using HCl, to which Tween 20 (Sigma-Aldrich) was diluted on the day of the experiment to a final concentration of 0.02%. ACE2-Fc and spike (Delta) recombinant proteins (for standard curve) were expressed respectively using transient or stable expression in CHO cells and purified in-house. Loading solution was prepared by adding the ACE2-Fc purified protein in matrix solution at a final concentration of

5 mg/L. Standard curves were prepared in matrix solution starting at 150 mg/L and then by performing 2-fold dilutions to obtain a total of eight dilutions. For the control, purified spike protein was diluted in matrix solution at a fixed concentration. Supernatants of static clone productions were diluted 1 in 3 in assay buffer. Quantification was performed by first capturing the ACE2-Fc on the Protein A probe (2 min), followed by a 5 s wash and capture of the spike protein in the diluted production samples for 2 min. The Octet-RED96 orbital shaker was set at 400 rpm and temperature to 30°C. The Octet acquisition program was used to generate the binding rate of samples. Five-parameter logistic fit was used to fit the standard curve. The standard curve was then used to interpolate the unknown samples response and calculate concentration.

2.10 | Analysis of glycans by monosaccharide analysis

Monosaccharides were analyzed after hydrolysis as reported previously (Farnós et al., 2020). In short, glycoproteins (25 µg) were hydrolyzed using sialidase (for sialic acid analysis) or TFA (for neutral sugar analysis). The samples were evaporated and/or diluted accordingly before injection on an HPAEC-PAD system.

2.11 | Surface plasmon resonance (SPR) binding assay

Binding affinity (K_D) of purified monomeric ACE2 to trimerized spike protein of SARS-CoV-2 (Delta) was determined using a Biacore T200 SPR instrument (Cytiva). ACE2-BAP (Biotin Acceptor Peptide) was produced and purified as described (Colwill et al., 2022), with an additional in vitro biotinylation step with BirA enzyme (MCLAB) to achieve full biotinylation of the BAP tag. The BirA reaction was performed according to the manufacturer's instructions, and the reaction mix was then passed on an IMAC column (Ni Sepharose Excel, Cytiva) to remove the enzyme. The eluted, biotinylated ACE2-BAP was buffer-exchanged into PBS using a NAP-25 desalting column. Production and purification of the spike proteins were carried out as described (Colwill et al., 2022). The SPR analysis was carried out in two steps, indirect capture of the spike protein via an in-house antibody against the human resistin trimerization partner immobilized onto the SPR surface, followed by flowing the ACE2 over top to generate binding sensorgrams. Samples were assayed at 25°C using PBS containing 0.05% Tween 20 (Teknova) with added 3.4 mM ethylenediaminetetraacetic acid (EDTA) and 0.05% Tween 20 as running buffer. The capture surface was generated using an in-house produced proprietary anti-resistin single-domain (VHH) antibody fused to a human IgG1 Fc. The antibody was diluted to 10 µg/mL in 10 mM sodium acetate immobilization buffer pH 4.5 (Cytiva) and immobilized to approximately 2000 RUs using the Immobilization Wizard for NHS/EDC amine coupling within the BiaControl instrument software. Spike proteins under analysis were diluted to 10 µg/mL in DPBS and captured onto the anti-resistin surface at 10 µL/min for 60 s. The ACE2 - spike protein interactions were assessed using single-cycle kinetics analysis with three concentrations, using a five-fold dilution from the top concentration of 200 nM. The ACE2 was injected at 50 µL/min over captured spike protein with a contact time of 150 s and a 600 s dissociation. Sensorgrams were double referenced to the blank anti-resistin sensor surface and analyzed for kinetic determination using a 1:1 binding model in BiaEvaluation software v3.0 (GE Healthcare).

2.12 | LC-MS/MS analysis

Forty micrograms of each spike protein was denatured and reduced with 0.1% Rapigest cleavable detergent (Waters) and 10 mM dithiothreitol (DTT) at 80°C for 10 min then alkylated with 37.5 mM iodoacetamide at room temperature (RT) in the dark for 30 min. The alkylation was quenched with further addition of DTT. The samples were then diluted to 400 µL (0.1 µg/µL) with 50 mM Tris-HCl, pH 8.0 and divided into two equal fractions. Trypsin (Promega) was added to one half and Endoproteinase Glu-C (Promega) was added to the other, each at a ratio 1:15 ratio (enzyme to spike protein). Both digests were incubated overnight at 37°C. The Rapigest detergent was cleaved in 0.5% trifluoroacetic acid at 37°C for 40 min and removed by centrifugation at 13,000 rpm for 20 min. The digests were analyzed on an Orbitrap Eclipse Tribrid mass spectrometer equipped with an electrospray ionization source (Thermo Scientific) and connected to an UltiMate 3000 nano-LC system (Thermo Scientific). Approximately 0.1 µg (≈0.7 pmoles) of each digest was injected onto a nanoACQUITY BEH 1.7 µm 100 µm × 100 mm C18 column (Waters) with a C18 PepMap100 5 µm × 3 mm trap (Thermo Scientific). Mobile phase A was 0.1% formic acid in ddH_2O, and mobile phase B was 0.1% formic acid in acetonitrile. Peptides were resolved using the following gradient: hold at 1% mobile phase for 5 min; 1%–45% mobile phase B over 15 min, 45%–95% mobile phase B over 6 min. The flow rate was 0.5 µL/min. MS spectra were acquired in the Orbitrap from 350 to 2000 *m/z* in positive electrospray ionization mode at 120 K resolution. The most intense ions (threshold = 1e6, dynamic exclusion = 25 s) were selected in the quadrupole for HCD-MS/MS (isolation window = 1.6 m/z) and a fixed HCD activation energy was selected based on peptide *m/z* and charge state using a decision tree. MS/MS spectra were acquired in the Orbitrap at 15 K resolution in profile mode. Cycle time was 1 s. Peptide MS/MS spectra were automatically searched against the Delta spike protein sequences using the Mascot™ search algorithm and with the following conditions: fixed modification: carbamidomethyl (C); variable modifications: deamidation (N/Q) and oxidation (M); peptide mass tolerance: 0.2 Da; fragment mass tolerance: 0.2 Da, enzyme: none. The MS/MS spectra were also searched manually to confirm identity of the N- and C-terminal peptide sequences.

2.13 | SEC-UPLC/MALS and differential scanning fluorimetry (DSF) analysis

SEC-UPLC/MALS analysis was performed as described in Stuible et al. (2021). DSF was used to determine in duplicate the melting curve of purified Delta variant spike samples. All samples were formulated in DPBS at pH 7.8. The protein concentration ranged from 0.7 to 1.3 mg/mL (corresponding to 1.7–3.1 µM of the spike trimer). A volume of 15 µL of each sample was placed in a 96-well qPCR plate (Applied Biosystems) to which was added 5 µL of a 40X Sypro Orange (Invitrogen) solution for a final dye concentration of 10X. The samples were mixed by pipetting up and down, and the plate was sealed with an optical adhesive cover (Applied Biosystems) and centrifuged for 5 min at 1000 g. Thermal melt curves were recorded using a QuantStudio 7 Flex real-time PCR instrument with a thermal gradient ramp from 25°C to 95°C at 0.9°C/min. Data were analyzed using the protein thermal shift software from Thermo Fisher.

2.14 | Transgene copy number analysis

A ddPCR assay was used to assess the copy number of genome-integrated spike transgenes in stably transfected CHO cells. Copy number was evaluated relative to the endogenous reference gene biglycan (BGN) which is present as a single copy in parental CHO^{2353} cells (data not shown). The transgene assay was based on duplex Taqman ddPCR (one primer/probe set for the reference gene and one for the transgene in each PCR reaction). Two regions of the transgene, one in the human resistin sequence at the C-terminus and other at the extreme N-terminus of the spike sequence (SmT1-N-term) were interrogated with separate primer/probe sets. The reference gene probe was labeled with FAM and the transgene probes were labeled with HEX. Genomic DNA was extracted from SmT1v3(Delta)-producing clones, the stable pool from which they were derived, and from parental CHO^{2353} cells (negative control) using the Monarch DNA purification kit (New England Biolabs). Before extraction, 5×10^6 cells were washed twice with cold PBS. Following extraction, the DNA concentration was measured by Nanodrop and 1 µg of extracted DNA was double-digested at 37°C for 60 min with 10 units each of EcoRI-HF and BamHI-HF (New England Biolabs) restriction enzymes to separate potential plasmid concatemers. The restriction enzymes were selected such that they did not cut either the reference or the target amplicons. The ddPCR reaction was set up according to the ddPCR supermix for probes (no dUTP) kit instructions (BioRad), using 25 ng of digested DNA, 18 µM of forward and reverse PCR primers and 5 µM of labeled probes. ddPCR was performed on the BioRad QX200 droplet digital PCR system. Briefly, 20 µL of the reaction mix was used to generate droplets with droplet generation oil for probes (BioRad). The droplets were then transferred and sealed into a PCR plate for thermal cycling using the following protocol: enzyme activation at 95°C for 5 min, 40 rounds of DNA denaturation (30 s), annealing (60 s), and extension (30 s) at 95°C, 60°C and 72°C respectively, followed by signal stabilization at 4°C and 90°C for 5 min each. The amplification signals were assessed using the QX200 droplet reader and the data was analyzed using QuantaSoft software (BioRad).

3 | RESULTS

Stable pools expressing spike proteins (nomenclature described in Section 2) were generated using the CHO^{2353} parental cell line which supports both constitutive and cumate-inducible protein expression, depending on the choice of plasmid vector (pTT81 and pTT241 for constitutive and inducible expression, respectively). We obtained consistently better yields of spike trimers from inducible pools. As shown in Figure 1, fed-batch productions of spike trimers for three variants (Alpha, Beta, and Delta variants) as well as a spike-scFv fusion protein gave protein titers 2- to 5-fold higher using cumate-inducible versus constitutive pools. Notably, differences between inducible and constitutive productivity are protein-dependent: we have found in some cases that constitutive pools can give similar or better expression levels than inducible pools (data not shown). However, because of the striking advantage of inducible expression for SARS-CoV-2 spike production, we used pTT241-transfected inducible pools for the remaining experiments described herein.

We generated multiple additional stable pools expressing SARS-CoV-2 spike variants fused to T1 or T2. Productivity was clearly variant-dependent, ranging from ~700 mg/L for the reference-strain and Delta variants to ~200 mg/L for Omicron (BA.1) and Alpha variants (all fused to T1), but the majority gave yields >400 mg/L (Figure 2). Importantly, although this level of productivity is lower

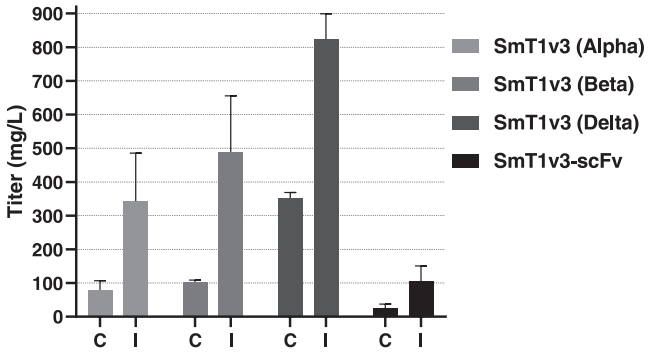

FIGURE 1 Inducible CHO^{2353} stable pools give better yields than constitutive pools for production of SARS-CoV-2 spike ectodomain protein constructs. Constructs corresponding to different SmT1v3 spike variant (Alpha, Beta, or Delta) ectodomains as well as reference-strain ectodomain fused to an scFv (SmT1v3-scFv) were produced using constitutive (C) or inducible (I) CHO^{2353} stable pools. Following transfection and pool selection with MSX, fed-batch productions were initiated. Supernatant samples were taken at 10 days post temperature shift and titers (spike concentrations) were determined by semiquantitative SDS-PAGE analysis using purified SmT1v3 as a standard. Data represent average ± SD of duplicate independent productions for each pool.

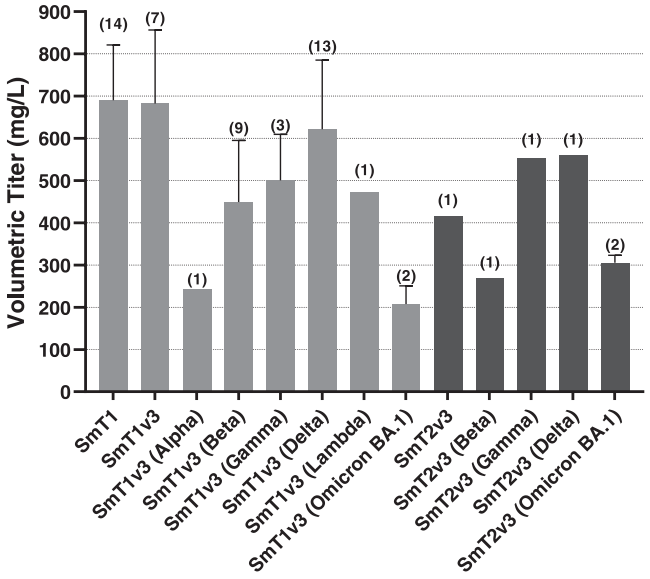

FIGURE 2 CHO[2353] inducible stable pools give yields >200 mg/L for spike ectodomains fused to resistin (T1) or foldon (T2) trimerization sequences. Evaluation of titers (recombinant spike construct concentrations in culture supernatants) from stable, inducible CHO pools following 10-day fed-batch productions. Titers were determined using a semi-quantitative SDS-PAGE analysis using purified SmT1v3 as standard. Error bars are shown (corresponding to SD) in cases where at least two independent productions were performed for a given pool. Number of independent productions is indicated in parenthesis over each group.

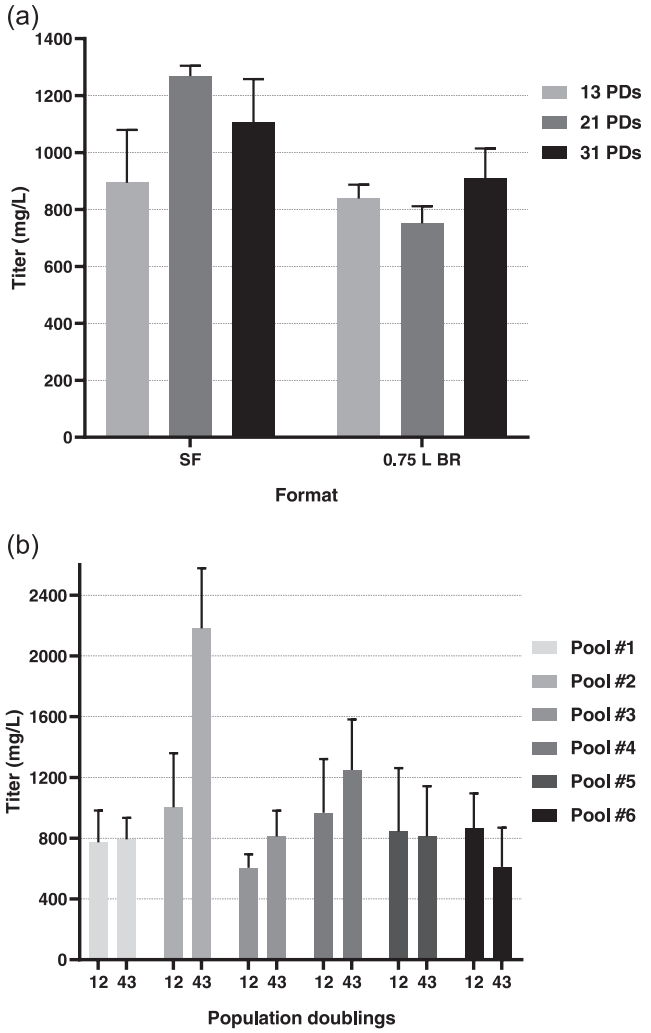

FIGURE 3 CHO[2353] stable pools expressing reference-strain (SmT1v3) and SmT1v3(Delta) proteins exhibit good expression stability after extended periods in culture. (a) Reference-strain spike protein expression was evaluated in shake flask (SF) and 0.75 L bioreactor formats (0.75 L BR) after maintenance of cells in culture for up to 31 population doublings (PDs). (b) Delta spike protein expression was evaluated in 6-well extradeepwell plates after maintenance of cells up to 43 population doublings. Thirteen days after initiating a fed-batch production, samples were taken for preparation of cleared culture supernatants. Titers were determined (two productions) using a semi-quantitative SDS-PAGE analysis using purified SmT1v3 as standard.

compared to other classes of recombinant proteins in CHO cells (e.g., monoclonal antibodies), it is significantly better than previously reported methods for production of recombinant spike protein, including in CHO cells and others like HEK293 and insect cells (Castro et al., 2021; Johari et al., 2021; Klumpp-Thomas et al., 2021; Mayrhofer et al., 2021; Schaub et al., 2021; Struble et al., 2022). Interestingly, when replicate pools expressing the same spike protein were generated (independent transfections/selections), the productivity of the pools was very similar (e.g., multiple pools expressing SmT1v3 (Delta) in Figure 3b), indicating that the differences in productivity of the pools generated for different variants (Figure 2) are not due to stochastic variability between experiments (e.g., plasmids could integrate at more or less favorable genomic loci in different experiments) but rather due to different variants being intrinsically easier or more difficult to express. We did not observe a consistent effect of the choice of trimerization sequence (T1 or T2) on productivity. During pool selection with MSX, cell viability for different spike constructs decreased to a minimum of 50%–70% for T1 constructs and ~50% for T2 constructs (see Supporting Information: Figure S1). Interestingly, this decrease in viability is more pronounced than usually observed for other types of recombinant proteins (e.g., antibodies), suggesting that spike proteins are more difficult to express (viability typically drops no lower than 85%–95% during MSX selection for antibody-expressing pools, data not shown). We also produced "Hexapro" spike constructs containing four additional prefusion-stabilizing proline mutations in the background of reference-strain spike sequence (Hsieh et al., 2020) from stable pools. In this case, cell viability dropped to only 70%–80% (see Supporting Information: Figure S1) and productivity was 0.9–1.5 g/L (data not shown), indicating that the Hexapro mutations do facilitate expression in CHO cells as reported previously for transient expression in HEK293 cells (Schaub et al., 2021). For all constructs, fed-batch productions in shake flasks were harvested at 10 days postinduction at which point they routinely attained ~15 million cells per mL with high cell viability of 98% on average (see Supporting Information: Figure S2).

To mimic the longer-duration culture required to generate cell banks and scale-up cultures to large volumes for bioreactor productions, pool stability was monitored by measuring spike productivity in shake flasks and in 0.75 L bioreactors after extended maintenance periods in culture. The productivity of a pool expressing SmT1v3 in shake flasks and bioreactors was not significantly different after 13, 21, or 31 population doublings (PD), averaging 800–1200 mg/L (Figure 3a). Among six independently generated pools expressing SmT1v3(Delta) (Figure 3b), five exhibited stable productivity after an extended period in culture (43 PD). For one pool (Pool #2, Figure 3b), productivity was unexpectedly increased after 43 PD; this indicates changes in the stably transfected cell population over time and would likely signal that product development with this pool should not be pursued. These results confirm the importance of verifying the stability in culture of CHO pools; however, despite being a mixed population of cells, it is clear that such pools do not systematically lose productivity during the time in culture required to expand them to scales necessary for mass production.

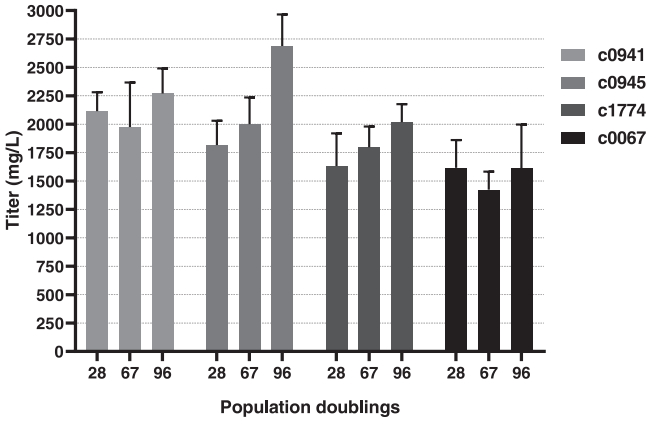

FIGURE 4 Productivity and expression stability of selected CHO^{2353}clones expressing SmT1v3(Delta) spike protein. Delta spike protein expression was evaluated by fed-batch production in 6-well extradeepwell plates after maintenance of cells in culture for up to 67 population doublings. Thirteen days after initiating production, samples were taken for preparation of cleared culture supernatants. Titers were determined twice on duplicate productions (except for T0 (28 PD): $n = 1$) using a semiquantitative SDS-PAGE analysis using purified SmT1v3 as standard. c0941, c0945, c1774, and c0067 are the names of clonal cell lines.

To compare purified spike products generated from stable pools and clones, we derived stable clones from a stable pool expressing SmT1v3(Delta) and characterized clones using our typical clone characterization platform process. Clones were screened and selected for their productivity and expression stability in culture for up to 67 PD. Fifteen out of eighteen top-expressing clones showed good expression stability (see Supporting Information: Figure S3). The best four selected clones expressed spike protein at 2.0–2.5 g/L (Figure 4); among these, clone c0945 showed a small but significant increase in productivity with increasing time in culture, indicating some degree of instability. Proteins produced by these clones were purified from culture supernatants using NGL COVID-19 Spike Protein Affinity Resin alongside material from pools expressing SmT1v3 from reference-strain, SmT1v3(Delta) and SmT2v3(Delta). Purified proteins were analyzed by SDS-PAGE and found to be highly pure and qualitatively comparable between pools and clones (Figure 5). Notably, one Delta pool produced detectable levels of a non-full-length product that was also captured by the spike affinity resin (Supporting Information: Figure S4); we believe this smaller protein is the result of a C-terminal truncation of the spike sequence, and it is the only example of a detectable,

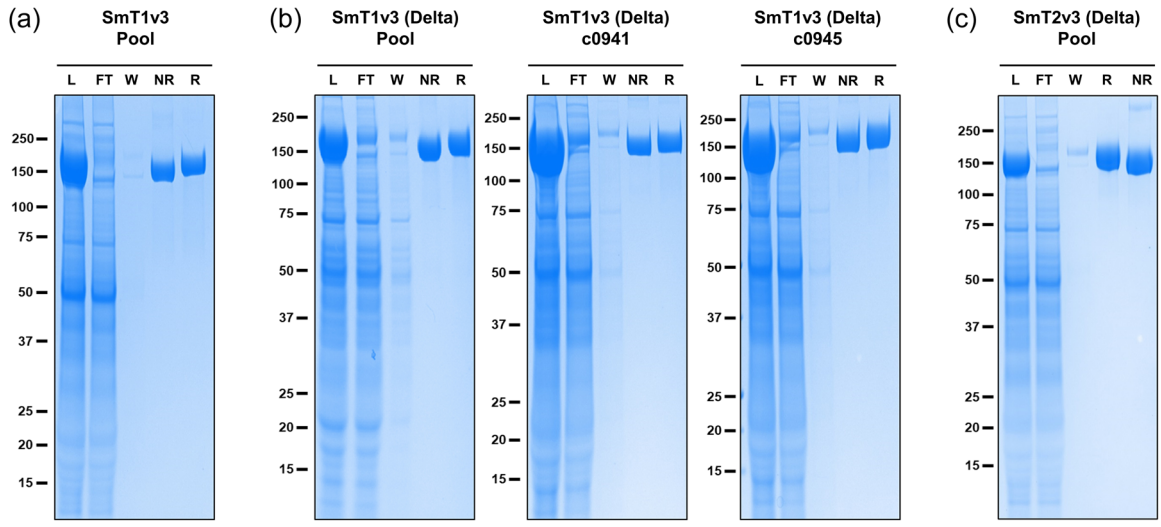

FIGURE 5 Reference-strain and Delta variant spike proteins purified from CHO^{2353} stable pools and clones exhibit similar size and purity. Cell culture supernatants from stable pool productions performed using SmT1v3 stable pool (a), a SmT1v3(Delta) stable pool and stable clones c0941 and c0945 (b), and a SmT2v3(Delta) stable pool (c) were purified using NGL COVID-19 Spike Protein Affinity Resin. Samples are from the load (L), flow-through (FT), wash (W), and elution steps were subjected to SDS-PAGE followed by staining with Coomassie Blue. Eluates were prepared in non-reducing (NR) and reducing (R) buffers.

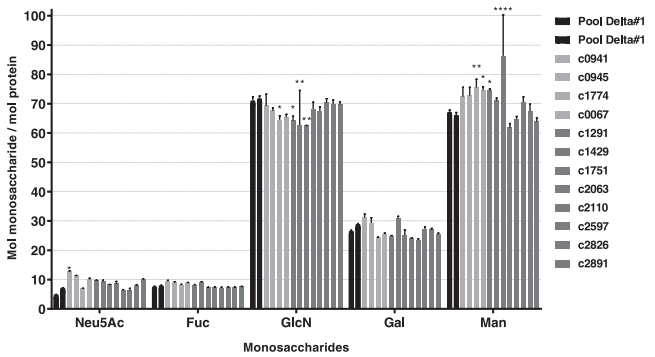

FIGURE 6 Glycans monosaccharide content for SmT1v3(Delta) spike proteins purified from CHO[2353] pools and clones. Purified spike proteins were analyzed for their *N*-acetylneuraminic acid (Neu5Ac) content after enzymatic hydrolysis, and in a separate assay, for their fucose (Fuc), glucosamine (GlcN), galactose (Gal), and mannose (Man) content after TFA hydrolysis. Both hydrolysates were injected on a high-performance anion exchange chromatography with pulsed amperometric detection (HPAEC-PAD) system. The data were analyzed using two-way analysis of variance, Tukey's multiple comparisons test, comparing the content of each monosaccharide type between variants. Statistical comparison was performed between pools and clones only (*$p < 0.05$, **$p < 0.01$, ****$p < 0.0001$). The data for pool represents the analysis of purified protein from two independent productions from the same Delta pool#1. The list of pools and cell lines on the right side of the figure corresponds to the bars on the graph from left to right.

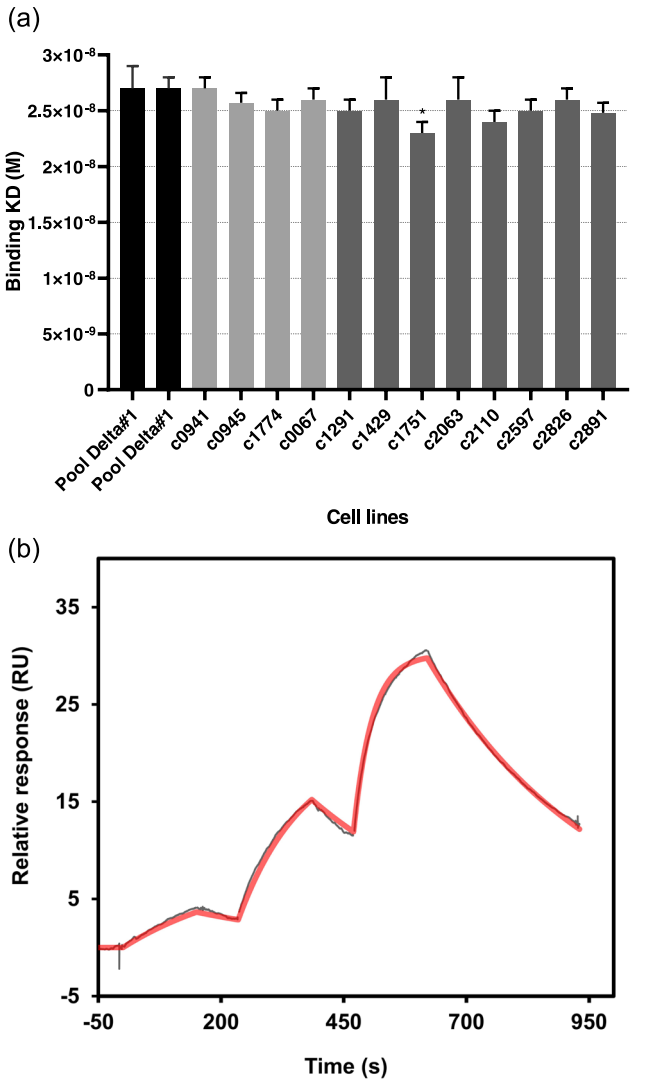

FIGURE 7 Binding to the cell-surface receptor ACE2 is similar for SmT1v3(Delta) spike proteins purified from stable pools and clones. (a) Dissociation equilibrium constants (K_D) were determined by surface plasmon resonance for purified spike proteins. Error bars correspond to SD of three independent injections (*$p < 0.05$). The data for pool represents the analysis of purified protein from two independent productions from the same Delta pool#1. (b) Representative sensorgram for sample of clone c0941.

truncated product expressed by any of the >30 spike pools we have generated so far.

To compare product quality in more detail, purified SmT1v3(Delta) proteins from pools and clones were analyzed using a panel of assays including glycan monosaccharide analysis, human ACE2 affinity determination by SPR, trimerization status and purity by SEC-UPLC coupled to MALS detector, identification of the N- and C-terminal sequences by LC-MS and thermal stability by DSF. As shown in Figure 6, proteins purified from several clones showed monosaccharide levels very similar to two independent productions from a Delta pool, even though some variability was detected between clones; notably, each SARS-CoV-2 spike protomer contains 21 occupied N-linked glycosylation sites (Sauvageau et al., submitted manuscript), for a potential of 63 N-glycans per trimer, making it technically challenging to assign glycan structures to specific sites by mass spectrometry-based methods. Similarly, binding affinity to the spike receptor ACE2 was found to be very similar between products of pools and clones by SPR, with protein from only a single clone (c1751) exhibiting an equilibrium dissociation constant (K_D) significantly different than the pool material (Figure 7). SEC-UPLC analysis also showed highly similar profiles for products from pools and clones (Figure 8). The main peak of the SEC-UPLC profile, corresponding to the trimeric spike, represented ~75%–80% of the product while the secondary peak, an hexameric form, represented ~15%–25% of the product. Representative SEC-UPLC profiles for SmT1v3 and SmT1v3(Delta) are shown in Supporting Information: Figure S5; the identity of the UPLC peaks was assigned based on multiangle light scattering (MALS) analysis, which estimated molecular weights of ~595 and ~1053 kDa, respectively, for trimers and hexamers. By LC-MS, N- and C-terminal peptide abundance was found to be nearly identical between products from pools and clones (see Supporting Information: Figure S6). 97.7%–99.1% of the tryptic N-terminal peptide sequences was 14-pQCVNLR-19 (where pQ is pyroglutamic acid) for all of the Delta spike proteins investigated. For the C-terminal peptide sequence, 98.5% to 99.1% was 1277-TTCHCQCAGMDWTGARCCRVQPG-1297, as expected. Finally, by DSF, all tested samples of pools and clones showed similar thermal stability with melting curves exhibiting two main transitions: the first one at ~44°C and the second at ~64°C

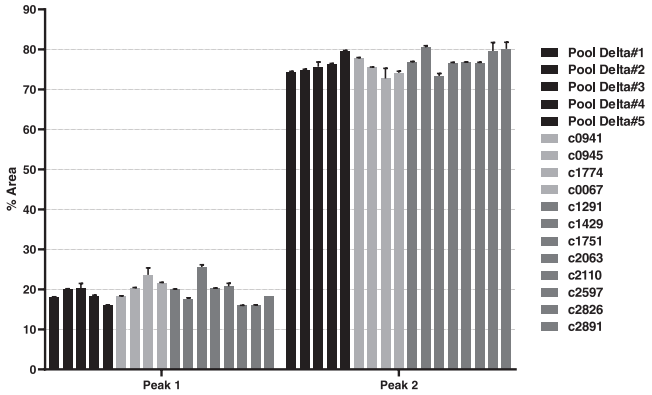

FIGURE 8 Purified SmT1v3(Delta) spike proteins from stable pools and clones exhibit similar proportions of trimer and hexamer species by size-exclusion chromatography (SEC)-UPLC. Purified proteins were separated by UPLC on a BEH450 SEC column. Protein elution was monitored by measuring UV absorbance of eluate. The % area of the two major peaks were plotted for each sample which was run in duplicate. Error bars correspond to SD of two independent injections. The list of pools and cell lines on the right side of the figure corresponds to the bars on the graph from left to right.

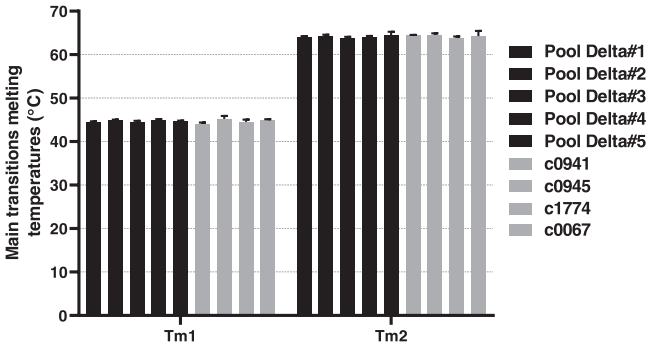

FIGURE 9 Thermal stability is similar for SmT1v3(Delta) purified from stable pools and clones. Purified proteins were analyzed in duplicate by differential scanning fluorimetry (DSF). The temperatures of the two principle melting transitions (T_m1 and T_m2) were determined from the DSF profiles as shown in Supporting Information: Figure S7. Error bars correspond to SD of two independent Tm calculations. The list of pools and cell lines on the right side of the figure corresponds to the bars on the graph from left to right.

(Figure 9), and overall melt curves were very similar (see Supporting Information: Figure S7). Together, this panel of orthogonal assays provides strong evidence of the high similarity of spike protein products derived from stable pools and clones.

Finally, we used a ddPCR-based method to compare the number of genome-integrated transgene copies in 11 top-producing clones expressing SmT1v3(Delta) versus the stable pool from which they were derived. As shown in Figure 10a, the pool contains an average

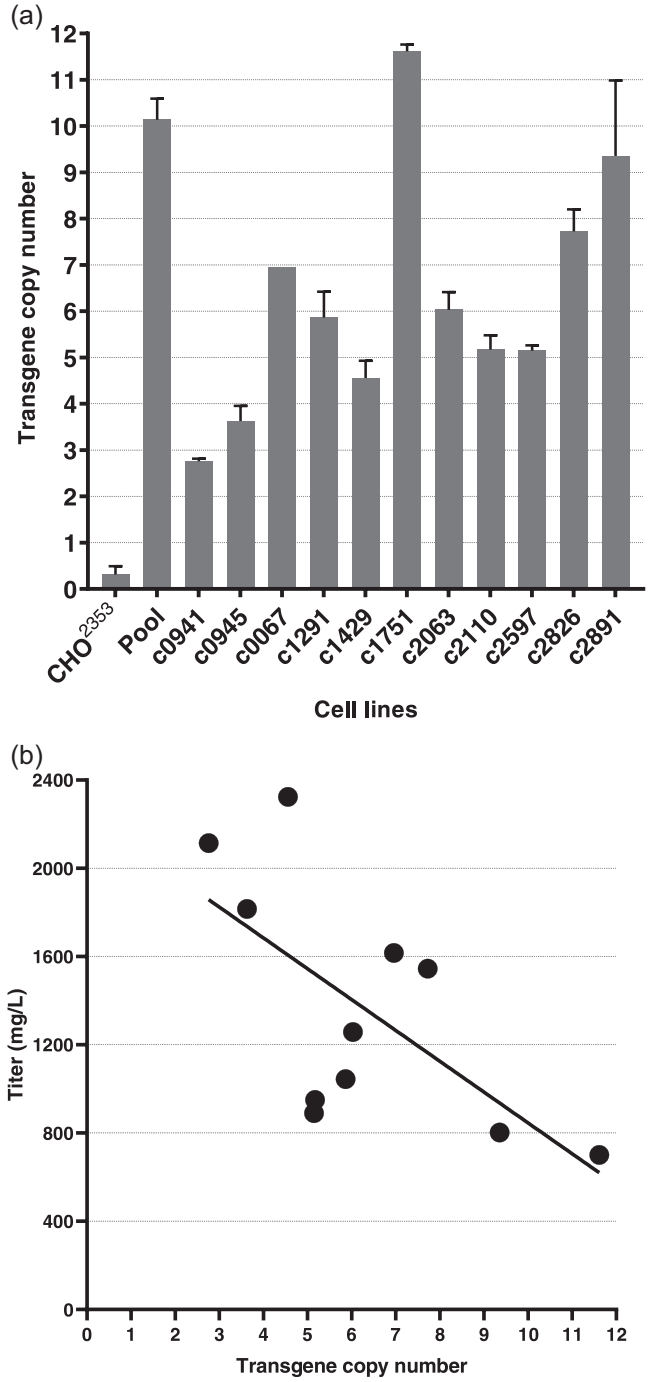

FIGURE 10 Comparison of transgene copy number and protein productivity for SmT1v3(Delta) clones. (a) Cell samples from stable pool and stable clones expressing SmT1v3(Delta) protein were analyzed for transgene copy number and compared to parental untransfected CHO^{2353} cell line as negative control. Average values are plotted with error bars corresponding to SD of two independent copy number determinations. (b) Titer obtained in fed-batch at T0 was plotted against average transgene copy number determined for each clone. Linear regression analysis (calculated R^2 of 0.42) was performed using GraphPad prism 8.2 software.

of ~10 transgene copies per cell, while 9 of 11 clones contain a significantly lower number of copies. Interestingly, although the number of data points is limited, there appears to be a negative correlation between copy number and protein productivity for these Delta clones: cells within a stable pool that have integrated a greater number of plasmid copies appear less likely to be among those producing the most recombinant protein (Figure 10b). A wide range of integrated transgene copy numbers has been reported in the literature for CHO pools and clones produced using a variety of methods, including many reports of high-producing cells with copy numbers similar to those reported here (Balasubramanian et al., 2018; Derouazi et al., 2006; Dhiman et al., 2020; Schmieder et al., 2022; Stadermann et al., 2022). Therefore, the copy number results we have obtained are not unexpected.

4 | DISCUSSION

For several years, stable CHO pools have been used extensively by our group for recombinant protein expression to support preclinical R&D activities; this mode of expression generally allows higher yields than transient gene expression with the possibility of using the same "platform" production conditions used for clonal cell lines. Notably, for these R&D projects, characterization of the expressed proteins has not always been comprehensive, and usually only a single pool is generated for each target. As described here, our focus on rapid production of diverse spike antigens during the COVID-19 pandemic required us to generate a large number of pools expressing different SARS-CoV-2 spike variants as well as replicate pools expressing the same proteins, all using the same pool selection protocol. This work provided a unique opportunity to confirm the robustness, and in particular the reproducibility, protein yield and product quality attributes of our stable pool platform. Furthermore, derivation of clonal cell lines from one of these stable pools confirmed the feasibility of bridging from the use of stable pools for early-phase clinical trials to clonal cell lines for later clinical stage manufacturing.

The random integration nature of the stable plasmid transfection approach used to generate our CHO pools dictates that integration of the plasmid into the host cell genome is a less well-controlled process than for targeted integration approaches (transposases/RMCE): genome-integrated plasmid sequences are expected to be found in different orientations, as concatemers and in truncated forms (Wurm & Petropoulos, 1994). Breakpoints between concatemerized plasmids as well as between plasmids and flanking genomic CHO DNA are also not predictable (Dhiman et al., 2020; Stadermann et al., 2022). Despite this, we have found production of non-full-length protein products from randomly integrated stable CHO pools to be quite infrequent: in the over 30 pools expressing spike proteins generated over the last 2 years, there was only a single pool expressing a truncated, discrete secreted product detected at low levels (shown in Supporting Information: Figure S4). For this pool, the truncated product was observable as a minor lower-molecular-weight protein band upon SDS-PAGE analysis of the purified product, corresponding to ~10% of the product as determined by densitometry analysis. If similar stable pool technology was used to produce material for clinical trials, we expect that the same basic analyses we have performed along with additional cell line characterization and analytical methods, as required by regulatory guidelines, would readily identify such rare cases and mitigate potential risks. Besides truncations, the mutation-prone nature of CHO cell genomes may also lead to emergence of internal point mutations in integrated transgene sequences; however, this risk should not be greater for pools generated by stable transfection (random integration) versus targeted integration. Current best practices for characterization of clonal cell lines during commercial cell line development should equally well identify issues with protein products produced from pools.

To date, CHO cell-based targeted integration platforms compatible with GMP manufacturing for clinical trials have been developed by a handful of large pharmaceutical companies (McGovern et al., 2022). In the case of targeted integration by RMCE, these platforms rely on parental CHO clones engineered with one or more integrated, exchangeable landing pads (Pascal et al., 2018); these require considerable resources for development and are not today a realistic option for early-stage companies. Likewise, for transposase-mediated integration, proprietary enzymes and vectors/sequences are necessary, and furthermore, often require engineered, proprietary GS-KO CHO cells for optimal performance (Agostinetto et al., 2022; Schmieder et al., 2022). We believe that the random integration approach we have used here to generate CHO pools is considerably more accessible, and its basic elements could be applied with any CHO cell line/expression vector using a widely used selection system (GS/MSX). The elements of our cell and plasmid vector technologies that permit cumate-inducible expression are proprietary (Poulain et al., 2017); we believe that the ability to turn off expression during MSX selection is advantageous for difficult-to-express proteins such as the SARS-CoV-2 spike, but for other proteins, constitutive expression using common viral or cellular promoters (e.g., hCMV) may give similar productivity and would not require proprietary technologies.

To enable future application of the CHO^{2353} stable pool method for rapid production of drug product for clinical trials, we have prepared fully characterized GMP-banked vials of these cells that can be transfected and selected under GMP conditions to minimize additional testing required before GMP production runs can take place. This approach removes both clone development and characterization steps (e.g., clone stability, identity, and adventitious agent testing) from the critical path to clinical trials. Notably, the most recent ICH Q5A(R2) draft guidelines open the possibility of omitting conventional in vitro and in vivo adventitious agent (AA) testing after transfection of well-characterized GMP CHO Master Cell Bank, in favor of more rapid next-generation sequencing (NGS) approaches. The expedited release of MCB for GMP production using NGS-based viral testing has been recently described (Tan et al., 2022; Zhang et al., 2021). We envision an accelerated workflow in which a GMP cell bank of stably transfected cells can be generated within just

4 weeks. After verification of product quality attributes and evaluation of pool stability, only rapid NGS-based AA testing would be required before a GMP bioreactor production run could commence. A conventional cell line development workflow can proceed in parallel without delaying initial clinical trials, generating well-characterized clonal cell lines from the GMP bulk pool. Our results obtained with a very limited set of clonal cell lines support the likelihood that the biochemical and biophysical characteristics of proteins produced by these clonal cell lines should be similar to those of the pool-derived material. A larger cell line development screening campaign would obviously further increase the chances of finding stable clones whose product is highly comparable to the pool product.

In the recent cases where purified material from non-clonal CHO cell lines was used for clinical trials, the molecules tested were all SARS-CoV-2-neutralizing monoclonal antibodies (Agostinetto et al., 2022; Tan et al., 2022; Xu et al., 2022; Zhang et al., 2021). Therefore, besides avoiding CHO clone generation steps, clinical development was also accelerated because monoclonal antibodies are a very well-understood class of protein therapeutics: previously established platform conditions for production, purification, formulation, and so on, could be applied with minimal additional development or validation. Although similarly shortened timelines would not have been possible for SARS-CoV-2 spike antigens at the onset of the pandemic, as these are highly complex new molecular entities, we believe that with the knowledge gained since then, this limitation may no longer apply. In particular, we have established a multi-step non-affinity purification method (including viral-inactivation) that is broadly effective for spike proteins from different SARS-CoV-2 variants as well as from distinct coronavirus families. Combined with the stable pool generation and production protocols that are similarly robust, protein subunit vaccine development and manufacturing for early clinical phase evaluation should be as rapid as neutralizing antibody development in response to future coronavirus outbreaks.

Apart from the shortened development timelines that could be enabled by non-clonal CHO-based methods, CHO cells have other advantages for production of viral vaccine antigens. CHO clones derived from our stable pools can produce SARS-CoV-2 spike protein with volumetric productivities of 2.0 g/L. With our typical purification yields (~30%), this would correspond to ~30,000 doses of vaccine antigen per litre of CHO culture medium (at 20 µg per dose). Combined with other advantages, including the native human-like glycosylation of spike protein produced in CHO cells as well as improved storage stability relative to mRNA vaccines, this could translate into improved immune response, improved logistics for worldwide vaccine distribution, and reduced manufacturing costs compared to currently approved vaccine options. Beyond COVID-19, CHO cells are by far the dominant mammalian expression system used to manufacture recombinant protein therapeutics, but only a very few licenced vaccines are produced in CHO: the Shingrix vaccine (GlaxoSmithKline), composed of recombinant glycoprotein E (gE) antigen from Varicella Zoster Virus (VZV) and the PreHevbrio vaccine (VBI vaccines), composed of the small (S), middle (pre-S2) and large (pre-S1) hepatitis B surface antigens, produced as enveloped virus-like particles (eVLP) are the only two licensed vaccines so far that we know of (Kim et al., 2021; Sucher et al., 2023; Walsh & Walsh, 2022). We thus believe that CHO cells should be carefully considered in the future as a viable option for production of a wide range of protein subunit vaccine antigens.

As non-clonal CHO-based approaches become a more widely accepted alternative to conventional cell line development workflows, we expect they could also see application beyond the response to virus outbreaks and other health emergencies. In particular, as these approaches develop a track record of safety and of producing material of similar quality and safety to that generated by clonal cell lines, we foresee an opportunity to accelerate and reduce the costs of clinical development by making it unnecessary to complete clone generation and characterization before initiating first-in-human trials. Especially for preclinical-stage biotech companies, this option would remove a significant obstacle, in terms of time and cost, to development of innovative and potentially life-saving protein-based therapeutics.

ACKNOWLEDGMENTS

We thank Brian Cass for reviewing the manuscript and Sam Williamson and Luc Tessier for support with the nano LC-MS platform. This project was funded by Canada's Pandemic Response Challenge Program. This is NRC publication #53682.

ORCID

Simon Joubert https://orcid.org/0009-0007-0405-8946
Matthew Stuible https://orcid.org/0009-0002-4403-0677
Yves Durocher https://orcid.org/0000-0002-2268-4111

REFERENCES

Agostinetto, R., Rossi, M., Dawson, J., Lim, A., Simoneau, M. H., Boucher, C., Valldorf, B., Ross-Gillespie, A., Jardine, J. G., Sok, D., Burton, D. R., Hassell, T., Broly, H., Palinsky, W., Dupraz, P., Feinberg, M., & Dey, A. K. (2022). Rapid cGMP manufacturing of COVID-19 monoclonal antibody using stable CHO cell pools. *Biotechnology and Bioengineering*, *119*(2), 663–666. https://doi.org/10.1002/bit.27995

Akache, B., Renner, T. M., Stuible, M., Rohani, N., Cepero-Donates, Y., Deschatelets, L., & Hill, J. J. (2022). Immunogenicity of SARS-CoV-2 spike antigens derived from Beta & Delta variants of concern. *NPJ Vaccines*, *7*(1), 1–7.

Akache, B., Renner, T. M., Tran, A., Deschatelets, L., Dudani, R., Harrison, B. A., Duque, D., Haukenfrers, J., Rossotti, M. A., Gaudreault, F., Hemraz, U. D., Lam, E., Régnier, S., Chen, W., Gervais, C., Stuible, M., Krishnan, L., Durocher, Y., & McCluskie, M. J. (2021). Immunogenic and efficacious SARS-CoV-2 vaccine based on resistin-trimerized spike antigen SmT1 and SLA archaeosome adjuvant. *Scientific Reports*, *11*(1), 21849.

Balasubramanian, S., Matasci, M., Kadlecova, Z., Baldi, L., Hacker, D. L., & Wurm, F. M. (2015). Rapid recombinant protein production from piggyBac transposon-mediated stable CHO cell pools. *Journal of Biotechnology*, *200*, 61–69. https://doi.org/10.1016/j.jbiotec.2015.03.001

Balasubramanian, S., Peery, R. B., Minshull, J., Lee, M., White, R., Kelly, R. M., & Barnard, G. C. (2018). Generation of high expressing Chinese hamster ovary cell pools using the Leap-In transposon system. *Biotechnology Journal*, *13*(10), 1700748.

Castro, R., Nobre, L. S., Eleutério, R. P., Thomaz, M., Pires, A., Monteiro, S. M., Mendes, S., Gomes, R. A., Clemente, J. J., Sousa, M. F. Q., Pinto, F., Silva, A. C., Freitas, M. C., Lemos, A. R., Akpogheneta, O., Kosack, L., Bergman, M. L., Duarte, N., Matoso, P., … Alves, P. M. (2021). Production of high-quality SARS-CoV-2 antigens: Impact of bioprocess and storage on glycosylation, biophysical attributes, and ELISA serologic tests performance. *Biotechnology and Bioengineering*, *118*(6), 2202–2219. https://doi.org/10.1002/bit.27725

Chisanga, M., Stuible, M., Gervais, C., L'Abbé, D., Cass, B., Bisson, L., & Boudreau, D. (2022). SERS-based assay for multiplexed detection of cross-reactivity and persistence of antibodies against the spike of the native, P. 1 and B. 1.617. 2 SARS-CoV-2 in non-hospitalised adults. *Sensors and Diagnostics*, *1*(4), 851–866.

Colwill, K., Galipeau, Y., Stuible, M., Gervais, C., Arnold, C., Rathod, B., Abe, K. T., Wang, J. H., Pasculescu, A., Maltseva, M., Rocheleau, L., Pelchat, M., Fazel-Zarandi, M., Iskilova, M., Barrios-Rodiles, M., Bennett, L., Yau, K., Cholette, F., Mesa, C., … Durocher, Y. (2022). A scalable serology solution for profiling humoral immune responses to SARS-CoV-2 infection and vaccination. *Clinical and Translational Immunology*, *11*(3), e1380. https://doi.org/10.1002/cti2.1380

Coulet, M., Kepp, O., Kroemer, G., & Basmaciogullari, S. (2022). Metabolic profiling of CHO cells during the production of biotherapeutics. *Cells*, *11*(12), 1929. https://doi.org/10.3390/cells11121929

Derouazi, M., Martinet, D., Besuchet Schmutz, N., Flaction, R., Wicht, M., Bertschinger, M., Hacker, D. L., Beckmann, J. S., & Wurm, F. M. (2006). Genetic characterization of CHO production host DG44 and derivative recombinant cell lines. *Biochemical and Biophysical Research Communications*, *340*(4), 1069–1077.

Dhiman, H., Campbell, M., Melcher, M., Smith, K. D., & Borth, N. (2020). Predicting favorable landing pads for targeted integrations in Chinese hamster ovary cell lines by learning stability characteristics from random transgene integrations. *Computational and Structural Biotechnology Journal*, *18*, 3632–3648.

Donaldson, J., Kleinjan, D. J., & Rosser, S. (2022). Synthetic biology approaches for dynamic CHO cell engineering. *Current Opinion in Biotechnology*, *78*, 102806. https://doi.org/10.1016/j.copbio.2022.102806

Durocher, Y., & Butler, M. (2009). Expression systems for therapeutic glycoprotein production. *Current Opinion in Biotechnology*, *20*(6), 700–707. https://doi.org/10.1016/j.copbio.2009.10.008

Fan, L., Rizzi, G., Bierilo, K., Tian, J., Yee, J. C., Russell, R., & Das, T. K. (2017). Comparative study of therapeutic antibody candidates derived from mini-pool and clonal cell lines. *Biotechnology Progress*, *33*(6), 1456–1462. https://doi.org/10.1002/btpr.2477

Farnós, O., Venereo-Sánchez, A., Xu, X., Chan, C., Dash, S., Chaabane, H., Sauvageau, J., Brahimi, F., Saragovi, U., Leclerc, D., & Kamen, A. A. (2020). Rapid high-yield production of functional SARS-CoV-2 receptor binding domain by viral and non-viral transient expression for pre-clinical evaluation. *Vaccines*, *8*(4), 654. https://doi.org/10.3390/vaccines8040654

Hall, C. A., Kravitz, R. H., Johnson, K. F., Sanek, N. A., Maiti, P., Ziemba, K. R., Liu, J., Andreev, D. O., Chrostowski, V. L., Collins, I. J., & Bleck, G. T. (2022). Shortening the biologics clinical timeline with a novel method for generating stable, high-producing cell pools and clones. *Biotechnology and Bioengineering*. https://doi.org/10.1002/bit.28323

Hsieh, C. L., Goldsmith, J. A., Schaub, J. M., DiVenere, A. M., Kuo, H. C., Javanmardi, K., Le, K. C., Wrapp, D., Lee, A. G., Liu, Y., Chou, C. W., Byrne, P. O., Hjorth, C. K., Johnson, N. V., Ludes-Meyers, J., Nguyen, A. W., Park, J., Wang, N., Amengor, D., … McLellan, J. S. (2020). Structure-based design of prefusion-stabilized SARS-CoV-2 spikes. *Science*, *369*(6510), 1501–1505. https://doi.org/10.1126/science.abd0826

Hu, Z., Hsu, W., Pynn, A., Ng, D., Quicho, D., Adem, Y., Kwong, Z., Mauger, B., Joly, J., Snedecor, B., Laird, M. W., Andersen, D. C., & Shen, A. (2017). A strategy to accelerate protein production from a pool of clones in Chinese hamster ovary cells for toxicology studies. *Biotechnology Progress*, *33*(6), 1449–1455. https://doi.org/10.1002/btpr.2467

Johari, Y. B., Jaffé, S. R. P., Scarrott, J. M., Johnson, A. O., Mozzanino, T., Pohle, T. H., Maisuria, S., Bhayat-Cammack, A., Lambiase, G., Brown, A. J., Tee, K. L., Jackson, P. J., Wong, T. S., Dickman, M. J., Sargur, R. B., & James, D. C. (2021). Production of trimeric SARS-CoV-2 spike protein by CHO cells for serological COVID-19 testing. *Biotechnology and Bioengineering*, *118*(2), 1013–1021. https://doi.org/10.1002/bit.27615

Joubert, S., Guimond, J., Perret, S., Malenfant, F., Elahi, S. M., Marcil, A., Parat, M., Gilbert, M., Lenferink, A. E. G., Baardsnes, J., & Durocher, Y. (2022). Production of afucosylated antibodies in CHO cells by coexpression of an anti-FUT8 intrabody. *Biotechnology and Bioengineering*, *119*, 2206–2220. https://doi.org/10.1002/bit.28127

Kim, K. S., Park, S. A., Wui, S. R., Ko, A., & Lee, N. G. (2021). Culture media optimization for Chinese hamster ovary cell growth and expression of recombinant varicella-zoster virus glycoprotein E. *Cytotechnology*, *73*(3), 433–445. https://doi.org/10.1007/s10616-021-00468-1

Klumpp-Thomas, C., Kalish, H., Drew, M., Hunsberger, S., Snead, K., Fay, M. P., Mehalko, J., Shunmugavel, A., Wall, V., Frank, P., Denson, J. P., Hong, M., Gulten, G., Messing, S., Hicks, J., Michael, S., Gillette, W., Hall, M. D., Memoli, M. J., … Sadtler, K. (2021). Standardization of ELISA protocols for serosurveys of the SARS-CoV-2 pandemic using clinical and at-home blood sampling. *Nature Communications*, *12*(1), 113. https://doi.org/10.1038/s41467-020-20383-x

Lam, C., Santell, L., Wilson, B., Yim, M., Louie, S., Tang, D., Shaw, D., Chan, P., Lazarus, R. A., Snedecor, B., & Misaghi, S. (2017). Taming hyperactive hDNase I: Stable inducible expression of a hyperactive salt- and actin-resistant variant of human deoxyribonuclease I in CHO cells. *Biotechnology Progress*, *33*(2), 523–533. https://doi.org/10.1002/btpr.2439

Matasci, M., Bachmann, V., Baldi, L., Hacker, D. L., De Jesus, M., & Wurm, F. M. (2011). Rapid recombinant protein production from pools of transposon-generated CHO cells. *BMC proceedings*, *5*(Suppl. 8), P34. https://doi.org/10.1186/1753-6561-5-s8-p34

Mayrhofer, P., Hunjadi, M., & Kunert, R. (2021). Functional trimeric SARS-CoV-2 envelope protein expressed in stable CHO cells. *Frontiers in Bioengineering and Biotechnology*, *9*, 779359. https://doi.org/10.3389/fbioe.2021.779359

McGovern, Ā. T., Salisbury, C. M., & Nyberg, G. B. (2022). The pandemic and resilience for the future: AccBio 2021. *Biotechnology Progress*, *38*(1), e3207. https://doi.org/10.1002/btpr.3207

Misaghi, S., Chang, J., & Snedecor, B. (2014). It's time to regulate: Coping with product-induced nongenetic clonal instability in CHO cell lines via regulated protein expression. *Biotechnology Progress*, *30*(6), 1432–1440. https://doi.org/10.1002/btpr.1970

Munro, T. P., Le, K., Le, H., Zhang, L., Stevens, J., Soice, N., Benchaar, S. A., Hong, R. W., & Goudar, C. T. (2017). Accelerating patient access to novel biologics using stable pool-derived product for non-clinical studies and single clone-derived product for clinical studies. *Biotechnology Progress*, *33*(6), 1476–1482. https://doi.org/10.1002/btpr.2572

Ong, E. C., Smidt, P., & McGrew, J. T. (2019). Limiting the metabolic burden of recombinant protein expression during selection yields

pools with higher expression levels. *Biotechnology Progress*, *35*(5), e2839. https://doi.org/10.1002/btpr.2839

Pascal, K. E., Dudgeon, D., Trefry, J. C., Anantpadma, M., Sakurai, Y., Murin, C. D., Turner, H. L., Fairhurst, J., Torres, M., Rafique, A., Yan, Y., Badithe, A., Yu, K., Potocky, T., Bixler, S. L., Chance, T. B., Pratt, W. D., Rossi, F. D., Shamblin, J. D., … Kyratsous, C. A. (2018). Development of clinical-stage human monoclonal antibodies that treat advanced Ebola virus disease in nonhuman primates. *The Journal of Infectious Diseases*, *218*(Suppl. 5), S612–S626.

Poulain, A., Mullick, A., Massie, B., & Durocher, Y. (2019). Reducing recombinant protein expression during CHO pool selection enhances frequency of high-producing cells. *Journal of Biotechnology*, *296*, 32–41. https://doi.org/10.1016/j.jbiotec.2019.03.009

Poulain, A., Perret, S., Malenfant, F., Mullick, A., Massie, B., & Durocher, Y. (2017). Rapid protein production from stable CHO cell pools using plasmid vector and the cumate gene-switch. *Journal of Biotechnology*, *255*, 16–27. https://doi.org/10.1016/j.jbiotec.2017.06.009

Rajendra, Y., Balasubramanian, S., McCracken, N. A., Norris, D. L., Lian, Z., Schmitt, M. G., Frye, C. C., & Barnard, G. C. (2017). Evaluation of piggyBac-mediated CHO pools to enable material generation to support GLP toxicology studies. *Biotechnology Progress*, *33*(6), 1436–1448. https://doi.org/10.1002/btpr.2495

Reyes, S. J., Durocher, Y., Pham, P. L., & Henry, O. (2022). Modern sensor tools and techniques for monitoring, controlling, and improving cell culture processes. *Processes*, *10*(2), 189. https://www.mdpi.com/2227-9717/10/2/189

Rodriguez-Conde, S., Inman, S., Lindo, V., Amery, L., Tang, A., Okorji-Obike, U., & Kortekaas, J. (2022). Suitability of transiently expressed antibodies for clinical studies: Product quality consistency at different production scales. *MAbs*, *14*(1), 2052228.

Rudi, E., Martin Aispuro, P., Zurita, E., Gonzalez Lopez Ledesma, M. M., Bottero, D., Malito, J., Gabrielli, M., Gaillard, E., Stuible, M., Durocher, Y., Gamarnik, A. V., Wigdorovitz, A., & Hozbor, D. (2022). Immunological study of COVID-19 vaccine candidate based on recombinant spike trimer protein from different SARS-CoV-2 variants of concern. *Frontiers in immunology*, *13*, 1020159. https://doi.org/10.3389/fimmu.2022.1020159

Scarcelli, J. J., Shang, T. Q., Iskra, T., Allen, M. J., & Zhang, L. (2017). Strategic deployment of CHO expression platforms to deliver Pfizer's monoclonal antibody portfolio. *Biotechnology Progress*, *33*(6), 1463–1467. https://doi.org/10.1002/btpr.2493

Schaub, J. M., Chou, C. W., Kuo, H. C., Javanmardi, K., Hsieh, C. L., Goldsmith, J., DiVenere, A. M., Le, K. C., Wrapp, D., Byrne, P. O., Hjorth, C. K., Johnson, N. V., Ludes-Meyers, J., Nguyen, A. W., Wang, N., Lavinder, J. J., Ippolito, G. C., Maynard, J. A., McLellan, J. S., & Finkelstein, I. J. (2021). Expression and characterization of SARS-CoV-2 spike proteins. *Nature Protocols*, *16*(11), 5339–5356. https://doi.org/10.1038/s41596-021-00623-0

Schmieder, V., Fieder, J., Drerup, R., Gutierrez, E. A., Guelch, C., Stolzenberger, J., Stumbaum, M., Mueller, V. S., Higel, F., Bergbauer, M., Bornhoefft, K., Wittner, M., Gronemeyer, P., Braig, C., Huber, M., Reisenauer-Schaupp, A., Mueller, M. M., Schuette, M., Puengel, S., … Fischer, S. (2022). Towards maximum acceleration of monoclonal antibody development: Leveraging transposase-mediated cell line generation to enable GMP manufacturing within 3 months using a stable pool. *Journal of Biotechnology*, *349*, 53–64. https://doi.org/10.1016/j.jbiotec.2022.03.010

Semba, C. P., Sugimoto, K., & Razavi, M. K. (2001). Alteplase and tenecteplase: Applications in the peripheral circulation. *Techniques in Vascular and Interventional Radiology*, *4*(2), 99–106. https://doi.org/10.1016/s1089-2516(01)90003-4

Srirangan, K., Loignon, M., & Durocher, Y. (2020). The use of site-specific recombination and cassette exchange technologies for monoclonal antibody production in Chinese Hamster ovary cells: Retrospective analysis and future directions. *Critical Reviews in Biotechnology*, *40*(6), 833–851.

Stadermann, A., Gamer, M., Fieder, J., Lindner, B., Fehrmann, S., Schmidt, M., Schulz, P., & Gorr, I. H. (2022). Structural analysis of random transgene integration in CHO manufacturing cell lines by targeted sequencing. *Biotechnology and Bioengineering*, *119*(3), 868–880.

Stark, F. C., Akache, B., Deschatelets, L., Tran, A., Stuible, M., Durocher, Y., & Harrison, B. A. (2022). Intranasal immunization with a proteosome-adjuvanted SARS-CoV2 spike protein-based vaccine is immunogenic and efficacious in mice & hamsters. bioRxiv. https://doi.org/10.1101/2022.03.02.482651.

Stocks, B., Thibeault, M.-P., Bates, J., Lord-Dufour, S., Gervais, C., Stuible, M., & Melanson, J. (2021). *SMT1-1: SARS-CoV-2 spike glycoprotein reference material | SMT1-1: Matériau de référence de la glycoprotéine spiculaire du SRAS-CoV-2*. National Research Council Canada.

Struble, L. R., Smith, A. L., Lutz, W. E., Grubbs, G., Sagar, S., Bayles, K. W., Radhakrishnan, P., Khurana, S., El-Gamal, D., & Borgstahl, G. E. O. (2022). Insect cell expression and purification of recombinant SARS-COV-2 spike proteins that demonstrate ACE2 binding. *Protein Science*, *31*(5), e4300. https://doi.org/10.1002/pro.4300

Stuible, M., Gervais, C., Lord-Dufour, S., Perret, S., L'Abbé, D., Schrag, J., St-Laurent, G., & Durocher, Y. (2021). Rapid, high-yield production of full-length SARS-CoV-2 spike ectodomain by transient gene expression in CHO cells. *Journal of Biotechnology*, *326*, 21–27. https://doi.org/10.1016/j.jbiotec.2020.12.005

Stuible, M., van Lier, F., Croughan, M. S., & Durocher, Y. (2018). Beyond preclinical research: Production of CHO-derived biotherapeutics for toxicology and early-phase trials by transient gene expression or stable pools. *Current Opinion in Chemical Engineering*, *22*, 145–151. https://doi.org/10.1016/j.coche.2018.09.010

Sucher, A. J., Sucher, B. J., & Chahine, E. B. (2023). PreHevbrio: A new 3-antigen hepatitis B vaccine for adults. *Annals of Pharmacotherapy*, *57*(3), 325–332. https://doi.org/10.1177/10600280221114469

Tan, K. W., Ji, P., Qian, Z., Gao, Q., Wang, S., Li, Q., Gu, M., Zhang, Q., Hou, C., Huang, Y., Lian, D., Wang, J., Zhang, Z., Zhang, S., Wu, J., & Zhou, W. (2022). Rapidly accelerated development of neutralizing COVID-19 antibodies by reducing cell line and CMC development timelines. *Biotechnology and Bioengineering*. https://doi.org/10.1002/bit.28302

Walsh, G., & Walsh, E. (2022). Biopharmaceutical benchmarks 2022. *Nature Biotechnology*, *40*(12), 1722–1760. https://doi.org/10.1038/s41587-022-01582-x

Wright, C., Alves, C., Kshirsagar, R., Pieracci, J., & Estes, S. (2017). Leveraging a CHO cell line toolkit to accelerate biotherapeutics into the clinic. *Biotechnology Progress*, *33*(6), 1468–1475. https://doi.org/10.1002/btpr.2548

Wurm, F. (2013). CHO quasispecies—Implications for manufacturing processes. *Processes*, *1*(3), 296–311. https://doi.org/10.3390/pr1030296

Wurm, F. M., & Petropoulos, C. J. (1994). Plasmid integration, amplification and cytogenetics in CHO cells: Questions and comments. *Biologicals*, *22*(2), 95–102.

Wurm, F. M., & Wurm, M. (2017). Cloning of CHO cells, productivity and genetic stability—A discussion. *Processes*, *5*(2), 20. https://doi.org/10.3390/pr5020020

Xu, G., Yu, C., Wang, W., Fu, C., Liu, H., Zhu, Y., Li, Y., Liu, C., Fu, Z., Wu, G., Li, M., Guo, S., Yu, X., Du, J., Yang, Y., Duan, M., Cui, Y., Feng, H., & Wang, L. (2022). Quality comparability assessment of a SARS-CoV-2-neutralizing antibody across transient, mini-pool-derived and single-clone CHO cells. *mAbs*, *14*(1), 2005507. https://doi.org/10.1080/19420862.2021.2005507

Ye, J., Alvin, K., Latif, H., Hsu, A., Parikh, V., Whitmer, T., Tellers, M., de la Cruz Edmonds, M. C., Ly, J., Salmon, P., & Markusen, J. F. (2010). Rapid protein production using CHO stable transfection pools. *Biotechnology Progress*, *26*(5), 1431–1437.

Zhang, Z., Chen, J., Wang, J., Gao, Q., Ma, Z., Xu, S., Zhang, L., Cai, J., & Zhou, W. (2021). Reshaping cell line development and CMC strategy for fast responses to pandemic outbreak. *Biotechnology Progress*, *37*(5), e3186. https://doi.org/10.1002/btpr.3186

SUPPORTING INFORMATION

Additional supporting information can be found online in the Supporting Information section at the end of this article.

How to cite this article: Joubert, S., Stuible, M., Lord-Dufour, S., Lamoureux, L., Vaillancourt, F., Perret, S., Ouimet, M., Pelletier, A., Bisson, L., Mahimkar, R., Pham, P. L., L'Ecuyer-Coelho, H., Roy, M., Voyer, R., Baardsnes, J., Sauvageau, J., St-Michael, F., Robotham, A., Kelly, J., … Durocher, Y. (2023). A CHO stable pool production platform for rapid clinical development of trimeric SARS-CoV-2 spike subunit vaccine antigens. *Biotechnology and Bioengineering*, 120, 1746–1761. https://doi.org/10.1002/bit.28387